Experimental and Theoretical Analysis of the Reorientational Dynamics of Fullerene C_{70} in Various Aromatic Solvents

R. M. Hughes,[†] P. Mutzenhardt,[‡] L. Bartolotti,[§] and A. A. Rodriguez*[,§]

Department of Biochemistry, Nanaline Duke Building, Duke University Medical Center, Durham, North Carolina 27710, Faculte des Sciences et Techniques, Laboratoire de Méthodologies RMN, BP 239, Université H. Poincaré, Boulevard des Aigillettes, F54506 Vandoeuvre-lés-Nancy Cedex, France, Department of Chemistry, East Carolina University, Greenville, North Carolina 27858

Received: January 2, 2008

A previous study of C_{70} in deuterated chlorobenzene generated evidence suggesting C_{70} was experiencing unique reorientational behavior at given temperatures. The present study explores the possibility that this behavior is present across other solvents. The ^{13}C spin−lattice relaxation rates for four carbon resonances in C_{70} were analyzed in benzene-d_6, chlorobenzene-d_5, and *o*-dichlorobenzene-d_4, and as a function of temperature, to probe the reorientational dynamics of this fullerene. Anisotropic behavior was observed at the lowest (283 K) and highest temperatures (323 K), isotropic diffusion was seen between 293 and 303 K, and quasi-isotropic at 313 K. When anisotropic motion was present, diffusion about the figure axis was seen to be higher than diffusion of the figure axis. Experimentally obtained diffusion coefficients generated reorientational correlation times that were in excellent agreement with experimental values. Theoretical predictions generated by a modified Gierer−Wirtz model provided acceptable predictions of the diffusion constants; with D_X usually being more closely reproduced and D_Z values generally being underestimated. Overall, the results indicate that the factors affecting rotational behavior are complex and that multiple solvent factors are necessary to characterize the overall motion of C_{70} in these solvents. Although a solvent's viscosity is normally sufficient to characterize the tumbling motion, the spinning motion is less sensitive to solvent viscosity but more responsive to solvent structure. The balance and collective influence of these factors ultimately determines the overall rotational behavior.

I. Introduction

In a previous study of the molecular dynamics of C_{70} in chlorobenzene-d_5 (CBZ), we found evidence suggesting C_{70}'s reorientational motion oscillated between anisotropic and isotropic behavior depending on the temperature.[1] To further explore the uniqueness of this behavior, we have expended our measurements to include C_{70} in benzene-d_6 (BZ) and in *o*-dichlorobenzene-d_4 (DCBZ).

Since the discovery of buckminsterfullerene (C_{60}) by Kroto and co-workers,[2−6] numerous other fullerenes have since been discovered. The common feature of these fullerenes is their all-carbon structure. This structure yields, provided a given allotrope has high enough symmetry, a relatively simple ^{13}C NMR spectrum which makes line assignments a relative simple task. Of particular interest to this communication is C_{70}, which because of its D_{5h} symmetry gives rise to 5 resonances. A second common feature of fullerenes is their spheroidal molecular shape, which makes them ideal for investigating molecular dynamics because many theoretical models contain the underlying presumption that a solute possesses this geometry.[7−13] Among the various experimental opportunities afforded by fullerenes, the possibility of studying the rotational dynamics of true spheroids is provided by its members.[14−22] To develop a more comprehensive understanding of the reorientational dynamics of these spheroids, we studied the temperature dependence of the ^{13}C spin−lattice relaxation rate of C_{70} in benzene-d_6, chlorobenzene-d_5, and *o*-dichlorobenzene-d_4. Our experimentally extracted correlation times allowed us to probe the rotational dynamics of C_{70} as well as allowing us to experimentally and theoretically evaluate the rotational diffusion constants D_Z and D_X. The calculated activation energies indicate that D_Z motion is preferred. To provide a theoretical explanation for the experimental observations, we applied a modified Gierer−Wartz model and found that this approach was able to provide acceptable predictions of the diffusion constants.

II. Experimental Section

C_{70} and the various solvents were purchased from the Aldrich Chemical Co.[23] A typical ^{13}C NMR spectrum of C_{70} showed the 5 unique resonances expected for this molecule. Carbon resonances were found at approximately 151, 146.5, 147.5, 145.5, and 131 ppm. These carbon resonances correspond to the carbons labeled in Figure 1. Resonances for carbons 1−4 were used for the analysis. Unfortunately, because of slight solvent peak interference and weak peak intensity of the carbon 5 resonance in chlorobenzene-d_5, which led to higher than acceptable error bars, it was not feasible to include the analysis of this peak across all solvents.

All solvents were received prepackaged in glass ampoules and were used as received. Optimum room-temperature concentrations of C_{70} in the solvents were calculated from published

* Corresponding author. Fax: (252) 328-6210. E-mail: rodriguezar@ecu.edu.
[†] Duke University Medical Center.
[‡] Université H. Poincaré.
[§] East Carolina University.

10.1021/jp800027j CCC: $40.75
Published on Web 04/11/2008

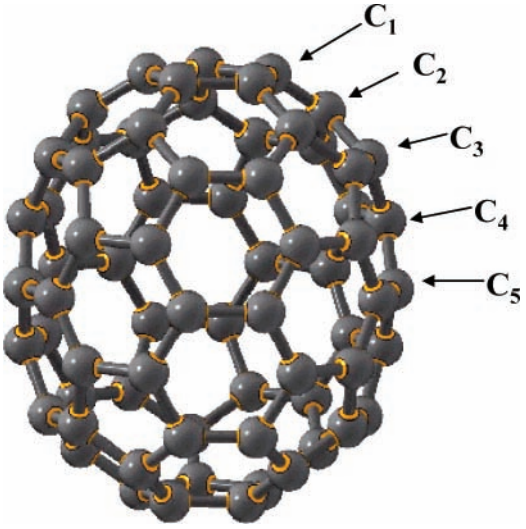

Figure 1. Carbon assignments in C_{70}. Carbon 1 (151 ppm), carbon 2 (146.5 ppm), carbon 3 (147.5 ppm), carbon 4 (145.5 ppm), and carbon 5 (131 ppm).

data.[24] Samples were contained in 5 mm tubes, connected to a vacuum line, and thoroughly degassed by several freeze−pump−thaw cycles to remove molecular oxygen. The tubes were then sealed under a vacuum.

^{13}C spin−lattice relaxation measurements were made on Varian instruments operating at 11.75 and 7.05 T. Experiments were conducted at five different temperatures (283, 293, 303, 313, and 323). The three higher sample temperatures were controlled by a FTS Systems heating apparatus (model TC-84) attached to the instruments, while the lower temperatures were controlled by a Kinetics Air-Jet cooling apparatus in conjunction with the FTS Systems heater. Temperature accuracy for these systems is ±0.1 K.

All relaxation times were obtained using the standard inversion−recovery pulse sequence as described in our earlier work.[16−20] The seven delay times used in the pulse sequence ranged in value from 0.1 to 1.5 times the estimated T_1. A delay time (D1) of approximately $5T_1$ was used between the transients. Each experiment used a minimum of 112 transients, resulting in an acquisition time of approximately 36 h.

III. Relaxation Mechanisms

It is now well-established that the only viable mechanisms for ^{13}C spin−lattice relaxation in fullerenes are the chemical shift anisotropy (CSA), R_1^{CSA}, and spin rotation interactions (SR), R_1^{SR}.[25−28] Therefore, the overall ^{13}C spin−lattice relaxation rate in C_{70} can be expressed as sum of these two mechanisms[29]

$$R_1 = \frac{1}{T_1} = R_1^{CSA} + R_1^{SR} \tag{1}$$

To obtain precise rotational information, the overall rate must be decomposed into its individual contributions which, when possible, can be accomplished by taking advantage of CSA's direct dependence and SR's independence to the applied magnetic field. Under extreme narrowing arguments, and assuming axial symmetry of the chemical shift tensor (CST), the CSA relaxation process is described by[30]

$$R_1^{CSA} = \left(\frac{2}{15}\right)\gamma_C{}^2 B_0{}^2 \Delta\sigma^2 \tau_C^{eff} \tag{2}$$

TABLE 1: Average Values for the Calculated Tensor Components, Chemical Shift Anisotropies, and the Chemical Shift Tensor (CST) Orientation of Carbons in C_{70}

carbon	σ_{xx} (ppm)	σ_{yy} (ppm)	σ_{zz} (ppm)	$\Delta\sigma$ (ppm)	θ (deg)
1	−33.56	−0.97	162.06	179.32	13.94
2	−24.35	0.04	164.65	176.81	51.99
3	−32.24	3.04	165.95	180.55	62.15
4	−22.30	−2.62	167.19	179.65	72.88
5	−8.62	11.56	181.77	180.30	90.00

where γ_c is the carbon magnetogyric ratio, B_o represents the field strength, $\Delta\sigma$ is the chemical shift anisotropy, and τ_C^{eff} is the effective reorientational correlation time. The chemical shift anisotropy is obtained from the three principal components (i.e., $\sigma_{zz} \geq \sigma_{yy} \geq \sigma_{xx}$) of the CST as defined by eq 3

$$\Delta\sigma = \sigma_{zz} - 0.5(\sigma_{xx} + \sigma_{yy}) \tag{3}$$

Although solid-state NMR measurements provide a direct method for determining the principal components, the approach can be experimentally challenging. This was experienced by Tycko and co-workers who attempted to evaluate the CST for the carbons in C_{70}.[31] The relative high noise in their measurements only permitted the determination of an average value of 200 ppm for each carbon in C_{70}. Alternatively, this information can be derived theoretically since recent advances in computational methods allow their determination with a high degree of accuracy.[32−39] Henceforth, we performed a quantum mechanical calculation of the chemical shielding tensors to generate the shielding anisotropy for the carbons in C_{70} and compared them to the experimentally derived values. For brevity, the calculation was performed with the Gaussian software package,[40] employing the B3LYP exchange-correlation energy density functional, the 6-31G* basis set,[41,42] and the gauge-independent atomic orbital method (GIAO).[43−46] A more thorough description of the approach is presented in ref 32. Although the experimental analysis was done on carbons 1−4, calculations were performed on all five carbons yielding values of 179.32, 176.81, 180.55, 179.65, and 180.30 ppm for carbons 1−5, respectively. Along with values for $\Delta\sigma$, the calculation yielded the necessary information to determine the orientation of the CST relative to the molecular axis, θ.[32] These results are given in Table 1. One quickly sees from this table that the shielding anisotropy varies little between the carbons and the values compare relatively well to the average found experimentally by Tycko.[31] It is interesting to note the similarity of $\Delta\sigma$ in C_{70} to C_{60}'s (178 ppm),[27] suggesting that anisotropies in other members of the fullerene family fall within this range.

The spin rotation interaction depends upon the symmetry of the molecule, its moments of inertia, and the spin rotation coupling constant, C. For a symmetric-top molecule, R_1^{SR} is proportional to[30]

$$R_1^{SR} = \frac{8\pi^2 I_{avg} kT}{\hbar^2} C_{avg}^2 \tau_J^{eff} \tag{4}$$

where I_{avg} and C_{avg}^2 are the average moments of inertia, $(2I_{xx} + I_{zz})/3$, and spin rotation coupling constant, $(2C_{xx}^2 + C_{zz}^2)/3$, respectively, whereas τ_J^{eff} is the effective angular momentum correlation time.

Substitution of relations 2 and 4 into eq 1 generate an expression that can easily be exploited to separate the CSA from the SR contributions

$$R_1 = \left(\frac{2}{15}\right)\gamma_C{}^2 B_0{}^2(\Delta\sigma)^2\tau_C^{eff} + \frac{8\pi^2 I_{avg} kT}{\hbar^2} C_{avg}^2 \tau_J^{eff} \qquad (5)$$

A fit of the overall relaxation rate against two or more field strengths (B_0^2), yields the magnitude of the CSA and SR contributions, as well as the value for τ_C^{eff}. Complete evaluation of τ_J^{eff} requires knowledge of C_{avg}, which is currently unavailable.

IV. Molecular Reorientation

Reorientation dynamics in liquids is normally described in terms of either diffusion constants, D_i, or reorientational correlation times, τ_c, because these two parameters are closely correlated. D_i is the diffusion rate about a given molecular axis, whereas τ_c is the time period required for the angular correlation function to decays to $1/e$ of its initial value.[47,48] These two parameters are related via[49]

$$\tau_C = \frac{1}{6D} \qquad (6)$$

A spherical molecule (e.g., C_{60}) experiencing isotropic type motion would be characterized by a single diffusion constant D or a single correlation time τ_c. On the other hand, symmetric-top molecules, such as C_{70}, are expected to exhibit anisotropic motion and therefore require two diffusion constants to characterize their overall motion. These two diffusion constants, D_Z and D_X, represent rotational diffusion about and of the top axis. This type of motion is now characterized by an effective reorientational correlation time that, in the limit of small-step diffusion, is given by[49]

$$\tau_C^{eff} = \frac{0.25(3\cos^2\theta - 1)^2}{6D_X} + \frac{3\sin^2\theta\cos^2\theta}{5D_X + D_Z} + \frac{0.75\sin^4\theta}{2D_X + 4D_Z} \qquad (7)$$

For CSA relaxation, θ is the orientation of the CST tensor relative to the molecular frame. In principle it is possible to determine D_Z and D_X for a symmetric-top molecule provided τ_C^{eff} and θ values are known for different nuclei in the molecule. In our case, this information is accessed via the resonances for carbons 1−4 of C_{70}. We employed our experimental correlation times, along with the Gaussian generated θ values, in eq 7 to simultaneously solve four equations (i.e., one for each carbon) and obtained the best-fit values for D_Z and D_X at each temperature.

V. Results and Discussion

The overall relaxation rates, along with the R_1^{CSA} and R_1^{SR} contributions, for carbons 1 thru 4 in C_{70} as a function of temperature, in the various solvents, and at the two field strengths are given in Tables 2−13. A cursory analysis of the relaxation rates for all carbons at 11.7 T indicate that the CSA mechanism plays a more significant role at the lower temperatures with a systematic increase in the SR contribution with rising temperature. A transition to the SR mechanisms is observed at approximately 313 K. On the other hand, the SR pathway dominates at 7.05 T. It is interesting to note that the relaxation rate for carbon 1 is always higher in all solvents suggesting a correlation between the effectiveness of the relaxation mechanism and the location of a nucleus relative to the symmetry axis.

TABLE 2: Spin−Lattice Relaxation Rates, Mechanistic Contributions, and Effective Reorientational Times for Carbon 1 of C_{70} in Benzene-d_6 at Various Temperatures

T (K)	$R_1 \times 10^{2a}$ (1/s)	$R_1 \times 10^{2b}$ (1/s)	$R_1^{CSA} \times 10^{2c}$ (1/s)	$R_1^{SR} \times 10^2$ (1/s)	τ_C^{eff} (ps)
283	6.80 (1.90)	2.52 (1.20)	6.69	0.11	25.0
293	3.94 (0.70)	1.63 (1.03)	3.61	0.33	13.5
303	3.49 (0.90)	1.61 (0.80)	2.94	0.55	11.0
313	4.16 (1.56)	2.75 (1.32)	2.20	1.96	8.1
323	5.50 (0.76)	4.34 (0.88)	1.81	3.69	6.8

[a] Relaxation rate at 11.7 T. [b] Relaxation rate at 7.05 T. Values in parenthesis represent standard deviations. [c] Chemical shift anisotropy contribution at 11.75 T.

TABLE 3: Spin−Lattice Relaxation Rates, Mechanistic Contributions, and Effective Reorientational Times for Carbon 2 of C_{70} in Benzene-d_6 at Various Temperatures

T (K)	$R_1 \times 10^{2a}$ (1/s)	$R_1 \times 10^{2b}$ (1/s)	$R_1^{CSA} \times 10^{2c}$ (1/s)	$R_1^{SR} \times 10^2$ (1/s)	τ_C^{eff} (ps)
283	3.74 (0.11)	1.49 (0.22)	3.52	0.22	13.5
293	3.56 (0.71)	1.54 (0.37)	3.16	0.40	12.1
303	3.30 (0.27)	1.53 (0.35)	2.77	0.53	10.6
313	4.20 (0.34)	2.90 (0.36)	2.03	2.17	7.8
323	6.03 (1.08)	4.88 (0.51)	1.80	4.23	6.9

[a] Relaxation rate at 11.7 T. [b] Relaxation rate at 7.05 T. Values in parenthesis represent standard deviations. [c] Chemical shift anisotropy contribution at 11.75 T.

TABLE 4: Spin−Lattice Relaxation Rates, Mechanistic Contributions, and Effective Reorientational Times for Carbon 3 of C_{70} in Benzene-d_6 at Various Temperatures

T (K)	$R_1 \times 10^{2a}$ (1/s)	$R_1 \times 10^{2b}$ (1/s)	$R_1^{CSA} \times 10^{2c}$ (1/s)	$R_1^{SR} \times 10^2$ (1/s)	τ_C^{eff} (ps)
283	3.70 (0.05)	1.45 (0.05)	3.52	0.18	12.9
293	3.51 (0.20)	1.49 (0.28)	3.16	0.35	11.6
303	3.20 (0.09)	1.54 (0.12)	2.59	0.61	9.6
313	4.01 (0.44)	2.80 (0.56)	1.89	2.12	7.0
323	5.88 (0.58)	4.97 (0.62)	1.38	4.50	5.2

[a] Relaxation rate at 11.7 T. [b] Relaxation rate at 7.05 T. Values in parenthesis represent standard deviations. [c] Chemical shift anisotropy contribution at 11.75 T.

The separated R_1^{CSA} contributions were used, along with eq 2, to extract the effective reorientational times, τ_C^{eff}, in the various solvents and temperatures. Values for τ_C^{eff} are given on the last columns of these tables. Since carbon nuclei in C_{70} are part of a rigid framework, τ_C^{eff} is a measure of the rotational motion of C_{70} itself. The observed differences in the rotational times for the carbons arise from their relative locations on the molecule giving them different angles of rotation in relation to the symmetry axis. In all cases one observes a decrease in the correlation times indicating faster rotational motion with rising temperature. Also, τ_C^{eff} for carbon 1 is always longer than the other carbons indicating slower displacement of this nuclear site

TABLE 5: Spin−Lattice Relaxation Rates, Mechanistic Contributions, and Effective Reorientational Times for Carbon 4 of C_{70} in Benzene-d_6 at Various Temperatures

T (K)	$R_1 \times 10^{2a}$ (1/s)	$R_1 \times 10^{2b}$ (1/s)	$R_1^{CSA} \times 10^{2c}$ (1/s)	$R_1^{SR} \times 10^2$ (1/s)	τ_C^{eff} (ps)
283	3.60 (0.23)	1.35 (0.28)	3.52	0.08	13.1
293	3.50 (0.11)	1.45 (0.51)	3.20	0.30	11.9
303	3.38 (0.09)	1.61 (0.21)	2.77	0.61	10.3
313	4.33 (0.29)	3.05 (0.32)	2.00	2.33	7.4
323	6.87 (0.31)	5.85 (0.55)	1.59	5.28	5.9

[a] Relaxation rate at 11.7 T. [b] Relaxation rate at 7.05 T. Values in parenthesis represent standard deviations. [c] Chemical shift anisotropy contribution at 11.75 T.

TABLE 6: Spin−Lattice Relaxation Rate, Mechanistic Contributions, and Effective Reorientational Times for Carbon 1 of C_{70} in Chlorobenzene-d_5 at Various Temperatures

T (K)	$R_1 \times 10^{2a}$ (1/s)	$R_1 \times 10^{2b}$ (1/s)	$R_1^{CSA} \times 10^{2c}$ (1/s)	$R_1^{SR} \times 10^2$ (1/s)	τ_C^{eff} (ps)
283	5.62 (0.28)	2.12 (0.34)	5.47	0.15	20.4
293	4.58 (0.37)	2.28 (0.87)	3.59	0.99	12.7
303	3.86 (0.40)	2.22 (0.90)	2.48	1.38	9.3
313	3.47 (0.52)	2.26 (0.82)	1.89	1.58	7.1
323	3.97 (1.04)	2.90 (1.24)	1.67	2.30	6.1

[a] Relaxation rate at 11.7 T. [b] Relaxation rate at 7.05 T. Values in parenthesis represent standard deviations. [c] Chemical shift anisotropy contribution at 11.75 T.

TABLE 7: Spin−Lattice Relaxation Rate, Mechanistic Contributions, and Effective Reorientational Times for Carbon 2 of C_{70} in Chlorobenzene-d_5 at Various Temperatures

T (K)	$R_1 \times 10^{2a}$ (1/s)	$R_1 \times 10^{2b}$ (1/s)	$R_1^{CSA} \times 10^{2c}$ (1/s)	$R_1^{SR} \times 10^2$ (1/s)	τ_C^{eff} (ps)
283	4.70 (0.60)	1.83 (0.90)	4.48	0.22	17.2
293	3.66 (0.07)	1.97 (0.17)	2.64	1.02	10.1
303	3.46 (0.22)	1.98 (0.61)	2.31	1.15	8.9
313	3.37 (0.03)	2.03 (1.40)	2.09	1.28	8.0
323	3.49 (0.85)	2.45 (0.55)	1.63	1.86	6.3

[a] Relaxation rate at 11.7 T. [b] Relaxation rate at 7.05 T. Values in parenthesis represent standard deviations. [c] Chemical shift anisotropy contribution at 11.75 T.

as C_{70} undergoes its reorientational motion. A comparison of the correlation times for carbon 1, at the lowest temperature, indicate the reorientational motion to be slowest in DCBZ but about equal in all solvents once the temperature rises. The differences between the correlation times for carbons 2−4 are not as drastic, with the differences narrowing with rising temperature. The data also show that the difference in the correlation times between solvents decreases with rising temperature and approaches an average value of approximately 5.6 ps at the highest temperature. This observation implies that thermal energy at 323 K is becoming sufficiently large to overcome solute−solvent related forces allowing for freer rotational motion.

TABLE 8: Spin−Lattice Relaxation Rate, Mechanistic Contributions, and Effective Reorientational Times for Carbon 3 of C_{70} in Chlorobenzene-d_5 at Various Temperatures

T (K)	$R_1 \times 10^{2a}$ (1/s)	$R_1 \times 10^{2b}$ (1/s)	$R_1^{CSA} \times 10^{2c}$ (1/s)	$R_1^{SR} \times 10^2$ (1/s)	τ_C^{eff} (ps)
283	3.70 (0.10)	1.49 (0.30)	3.45	0.25	12.7
293	3.60 (0.06)	1.59 (0.16)	3.14	0.46	11.6
303	3.21 (0.29)	1.64 (0.59)	2.45	0.76	9.0
313	2.69 (0.35)	1.65 (0.77)	1.63	1.06	6.0
323	2.83 (0.43)	2.07 (0.32)	1.19	1.64	4.4

[a] Relaxation rate at 11.7 T. [b] Relaxation rate at 7.05 T. Values in parenthesis represent standard deviations. [c] Chemical shift anisotropy contribution at 11.75 T.

TABLE 9: Spin−Lattice Relaxation Rate, Mechanistic Contributions, and Effective Reorientational Times for Carbon 4 of C_{70} in Chlorobenzene-d_5 at Various Temperatures

T (K)	$R_1 \times 10^{2a}$ (1/s)	$R_1 \times 10^{2b}$ (1/s)	$R_1^{CSA} \times 10^{2c}$ (1/s)	$R_1^{SR} \times 10^2$ (1/s)	τ_C^{eff} (ps)
283	4.43 (0.17)	1.78 (0.50)	4.14	0.29	15.4
293	4.02 (0.33)	1.80 (0.43)	3.47	0.55	12.9
303	3.61 (0.15)	1.90 (0.35)	2.67	0.94	9.9
313	2.99 (0.13)	1.79 (0.53)	1.88	1.11	7.0
323	3.45 (0.28)	2.52 (0.58)	1.45	2.00	5.4

[a] Relaxation rate at 11.7 T. [b] Relaxation rate at 7.05 T. Values in parenthesis represent standard deviations. [c] Chemical shift anisotropy contribution at 11.75 T.

TABLE 10: Spin−Lattice Relaxation Rates, Mechanistic Contributions, and Effective Reorientational Times for Carbon 1 of C_{70} in o-Dichlorobenzene-d_4 at Various Temperatures

T (K)	$R_1 \times 10^{2a}$ (1/s)	$R_1 \times 10^{2b}$ (1/s)	$R_1^{CSA} \times 10^{2c}$ (1/s)	$R_1^{SR} \times 10^2$ (1/s)	τ_C^{eff} (ps)
283	7.04 (0.28)	2.55 (0.55)	7.02	0.02	26.2
293	5.06 (0.39)	2.75 (0.59)	3.61	1.45	13.5
303	4.57 (0.76)	2.81 (0.86)	2.75	1.82	10.3
313	4.93 (0.29)	3.40 (0.58)	2.39	2.54	8.9
323	6.12 (0.90)	4.79 (1.01)	2.18	3.94	7.8

[a] Relaxation rate at 11.7 T. [b] Relaxation rate at 7.05 T. Values in parenthesis represent standard deviations. [c] Chemical shift anisotropy contribution at 11.75 T.

Columns 2 and 3 of Tables 14−16 contain values for the diffusion coefficients D_X and D_Z, obtained by using experimentally obtained correlation times, τ_C^{eff}, the relative angles of C_1−C_4 to the symmetry axis, and simultaneously solving eq 7. In benzene, one sees that at 283 K, the diffusion about the top axis, D_Z, is significantly larger than the motion of the top axis, D_X. Between 293 and 313 K, one observes quasi-isotropic type reorientation within this temperature range. At 323 K, the

TABLE 11: Spin−lattice Relaxation Rates, Mechanistic Contributions, and Effective Reorientational Times for Carbon 2 of C_{70} in o-Dichlorobenzene-d_4 at Various Temperatures

T (K)	$R_1 \times 10^{2a}$ (1/s)	$R_1 \times 10^{2b}$ (1/s)	$R_1^{CSA} \times 10^{2c}$ (1/s)	$R_1^{SR} \times 10^2$ (1/s)	τ_C^{eff} (ps)
283	4.30 (0.22)	1.65 (0.32)	4.14	0.16	15.9
293	4.03 (0.28)	1.73 (0.65)	3.59	0.44	13.8
303	3.69 (0.57)	1.80 (0.22)	2.95	0.74	11.3
313	3.78 (0.16)	2.51 (0.25)	1.98	1.80	7.6
323	5.19 (0.11)	4.10 (0.68)	1.70	3.49	6.5

[a] Relaxation rate at 11.7 T. [b] Relaxation rate at 7.05 T. Values in parenthesis represent standard deviations. [c] Chemical shift anisotropy contribution at 11.75 T.

TABLE 12: Spin−Lattice Relaxation Rates, Mechanistic Contributions, and Effective Reorientational Times for Carbon 3 of C_{70} in o-Dichlorobenzene-d_4 at Various Temperatures

T (K)	$R_1 \times 10^{2a}$ (1/s)	$R_1 \times 10^{2b}$ (1/s)	$R_1^{CSA} \times 10^{2c}$ (1/s)	$R_1^{SR} \times 10^2$ (1/s)	τ_C^{eff} (ps)
283	4.33 (0.14)	1.57 (0.34)	4.31	0.02	15.9
293	4.08 (0.12)	1.69 (0.56)	3.73	0.35	13.7
303	3.60 (0.06)	1.78 (0.14)	2.84	0.76	10.5
313	3.67 (0.59)	2.28 (0.64)	2.17	1.50	8.0
323	4.19 (0.36)	3.11 (0.77)	1.69	2.50	6.2

[a] Relaxation rate at 11.7 T. [b] Relaxation rate at 7.05 T. Values in parenthesis represent standard deviations. [c] Chemical shift anisotropy contribution at 11.75 T.

TABLE 13: Spin−Lattice Relaxation Rates, Mechanistic Contributions, and Effective Reorientational Times for Carbon 4 of C_{70} in o-Dichlorobenzene-d_4 at Various Temperatures

T (K)	$R_1 \times 10^{2a}$ (1/s)	$R_1 \times 10^{2b}$ (1/s)	$R_1^{CSA} \times 10^{2c}$ (1/s)	$R_1^{SR} \times 10^2$ (1/s)	τ_C^{eff} (ps)
283	4.96 (0.67)	1.88 (0.43)	4.81	0.15	17.9
293	4.24 (0.22)	1.79 (0.49)	3.83	0.41	14.2
303	4.00 (0.14)	1.98 (0.51)	3.16	0.84	11.7
313	4.24 (0.73)	2.77 (0.60)	2.30	1.94	8.5
323	4.36 (0.30)	3.29 (0.58)	1.67	2.69	6.2

[a] Relaxation rate at 11.7 T. [b] Relaxation rate at 7.05 T. Values in parenthesis represent standard deviations. [c] Chemical shift anisotropy contribution at 11.75 T.

reorientation reverts back to anistropic type motion, suggesting an unequal and preferred activation of the D_Z type motion. An Arrhenius fit of the diffusion constants yielded activation energies of 25.2 and 5.9 kJ/mol for D_X and D_Z type motions, respectively, indicating a clear preference for the spinning motion. The close agreement between experimental and calculated correlation times, τ_C^{eff} (cal), in Table 14 signifies that the extracted diffusion constants are providing an acceptable description of the overall reorientational motion of C_{70} in this solvent.

Table 15 contains diffusion information for C_{70} in CBZ. From this table, one sees that,at the lowest temperature, diffusion about the top axis is approximately twice as fast as motion of the top axis. Because pure inertial effects would predict the diffusion constants to differ only by about 15%, this observation suggests that the tumbling motion is more sensitive to solvent effects (e.g., solvent displacement) and, consequently, is slower than expected. A 10° rise in temperature has no effect on D_Z but causes a noticeable increase in D_X. Although this observation is unusual, it would imply that the increased thermal energy allows C_{70} to more efficiently displace solvent molecules during its tumbling motion. The ratio of the diffusion constants is more in line with inertial effects being the primary factor affecting the diffusional motion at this temperature. Beginning at 293 K and progressing to 313 K, the differences between D_Z and D_X are within experimental error indicating that C_{70} is now experiencing isotropic reorientation. Surprisingly, however, the motion is predicted to once again become anisotropic at the highest temperature. This latter prediction is highly anomalous and could be resulting from errors propagated from the experimental measurements since error bars at this temperature were higher. An Arrhenius fit of the diffusion constants as a function of inverse temperature yielded activation energies of 21.9 and 17.0 kJ/mol for the D_X and D_Z type motions, respectively, indicating a higher retarding force, 4.9 kJ higher, for the tumbling motion. Table 15 also shows the close agreement between experimental and calculated correlation times, τ_C^{eff} (cal), which shows that the extracted diffusion constants are providing an suitable description of the reorientational motion of C_{70} in CBZ.

A comparison of the diffusion constants for C_{70} in BZ and CBZ shows that the D_Z component remains relatively unchanged across both solvents, whereas a slight increase in D_X is observed in the more viscous CBZ. This behavior may result from a balance of several factors (e.g., viscosity, intermolecular forces, solvent structure, etc.) affecting the tumbling motion of C_{70}. Since solute−solvent interactions in fullerenes have been shown experimentally to decrease in magnitude in the order of BZ > CBZ > DCBZ[50,51] and calculated free-volume increase in the order of BZ > CBZ > DCBZ,[52] the data suggest that solvent structure plays an important role in this observation.

The diffusion information for C_{70} in DCBZ is given in Table 16. Analysis of these data show that the reorientational motion is slightly anisotropic at 283 K, with $D_Z \geq D_X$. The motion becomes isotropic between 293 and 303 K and reverts back to anisotropic at the two highest temperatures. This unusual behavior suggests that a balance of several interrelated factors, (e.g., solvent structure, bulk viscosity, thermal energy, etc) are determining the molecular dynamics of this fullerene. An Arrhenius fit of these diffusion constants generated activation energies of 22.8 and 14.1 kJ/mol for D_X and D_Z type motions, respectively. The last columns in Table 16 illustrate the agreement between experimental and calculated correlation times which suggests that the fitted diffusion constants provide a satisfactory description of the reorientational motion of C_{70} in this DCBZ.

A comparison of the diffusion constants for C_{70} in this solvent with those found in BZ and CBZ generates some interesting observations. Because the spinning rate, D_Z, is generally seen to be slightly lower in this more viscous solvent than in BZ or CBZ, this observation suggests that the viscosity parameter is not the dominant factor giving rise to the observed spinning behavior of C_{70} in these solvents. It appears that in CBZ and DCBZ, the balance lies between the strength of the intermo-

TABLE 14: Predicted Rotational Diffusion Constants and Experimental and Calculated Correlation Times for the Different Carbons at Various Temperatures for C_{70} in Benzene-d_6

			carbon 1		carbon 2		carbon 3		carbon 4	
T (K)	$D_X \times 10^{-10}$ (1/s)	$D_Z \times 10^{-10}$ (1/s)	τ_C^{eff} (ps)	τ_C^{eff} (cal) (ps)	τ_C^{eff} (ps)	τ_C^{eff} (cal) (ps)	τ_C^{eff} (ps)	τ_C^{eff} (cal) (ps)	τ_C^{eff} (ps)	τ_C^{eff} (cal) (ps)
283	0.6	1.6	25.0	25.0	13.5	14.1	12.9	12.8	13.1	12.5
293	1.2	1.7	13.5	13.5	12.1	12.2	11.6	11.9	11.9	11.6
303	1.5	1.9	11.0	11.0	10.6	10.3	9.6	10.1	10.3	10.0
313	2.0	2.7	8.1	8.2	7.8	7.6	7.0	7.4	7.4	7.3
323	2.4	3.5	6.8	6.9	6.9	6.2	5.2	5.9	5.9	5.8

TABLE 15: Predicted Rotational Diffusion Constants and Experimental and Calculated Correlation Times for the Different Carbons at Various Temperatures for C_{70} in Chlorobenzene-d_5

			carbon 1		carbon 2		carbon 3		carbon 4	
T (K)	$D_X \times 10^{-10}$ (1/s)	$D_Z \times 10^{-10}$ (1/s)	τ_C^{eff} (ps)	τ_C^{eff} (cal) (ps)	τ_C^{eff} (ps)	τ_C^{eff} (cal) (ps)	τ_C^{eff} (ps)	τ_C^{eff} (cal) (ps)	τ_C^{eff} (ps)	τ_C^{eff} (cal) (ps)
283	0.8	1.6	20.4	20.5	17.2	15.9	12.7	15.0	15.4	14.4
293	1.4	1.6	12.7	12.1	10.1	11.8	11.6	11.7	12.9	11.6
303	1.8	1.8	9.3	9.3	8.9	9.3	9.0	9.3	9.9	9.3
313	2.3	2.6	7.1	7.3	8.0	7.0	6.0	6.9	7.0	6.9
323	2.6	3.9	6.2	6.3	6.3	5.5	4.4	5.3	5.4	5.2

TABLE 16: Predicted Rotational Diffusion Constants and Experimental and Calculated Correlation Times for the Different Carbons at Various Temperatures for C_{70} in *o*-Dichlorobenzene-d_4

			carbon 1		carbon 2		carbon 3		carbon 4	
T (K)	$D_X \times 10^{-10}$ (1/s)	$D_Z \times 10^{-10}$ (1/s)	τ_C^{eff} (ps)	τ_C^{eff} (cal) (ps)	τ_C^{eff} (ps)	τ_C^{eff} (cal) (ps)	τ_C^{eff} (ps)	τ_C^{eff} (cal) (ps)	τ_C^{eff} (ps)	τ_C^{eff} (cal) (ps)
283	0.6	1.1	26.1	26.1	15.9	17.7	15.9	16.2	17.9	15.6
293	1.2	1.2	13.5	13.8	13.8	13.8	13.7	13.8	14.2	13.8
303	1.5	1.5	10.3	10.9	11.3	10.9	10.5	10.9	11.7	10.9
313	1.9	2.3	8.9	8.7	7.6	8.2	8.0	8.1	8.5	8.0
323	2.1	3.6	7.8	7.7	6.5	6.6	6.2	6.3	6.2	6.1

lecular forces and solvent structure. Because the free volume is greater in DCBZ, this suggests that the available free space is more important than solute−solvent interactions in determining the spinning freedom of C_{70} in these two solvents. The tumbling motion, D_X, is slowest in DCBZ: consistent with the higher viscosity of this solvent. One must however be cautious of oversimplifying this observation, because as we saw for the other type of motion, other solvent-related factors are also present.

VI. Comparison with Theoretical Predictions

The anisotropic rotational diffusion, D_i, of a spheroid is regularly analyzed via models derived from the Stokes−Einstein−Debye (SED) diffusional equations.[7] Using the SED theory as its basis, Perrin was able to derive expressions for diffusion about and of the top axes; D_Z and D_X, respectively.[53] These are given as

$$D_i = \left(\frac{1}{f_i}\right)D_S = \left(\frac{1}{f_i}\right)\left(\frac{kT}{8\pi r_i^3 \eta}\right) \tag{8}$$

where f_i is a friction coefficient associated with the spinning or tumbling motion and depends on the axial ratio, ρ, of the spheroid in question. The solute's average molecular radius is given by r, η is the solvent bulk viscosity, and kT corresponds to the thermal energy.

We recently applied the Perrin,[53] Hu-Zwanzig,[12] Gillen and Griffiths,[54] and the Gierer−Wirtz[8] models in the study of C_{70} in chlorobenzene and found that, of these models, only a modified Gierer−Wirtz approach generated rates that were consistent with our experimental values.[1] Key features of the Gierer−Wirtz approach is the "sticking factor," σ_{GW}, a solvation number, C_o, and the concept of microviscosity effects on reorientational motion. According to this model, the friction coefficient, f_{GW}, is a function of the solvent-to-probe molecular volume ratio (i.e., V_S/V_P) and is defined as[55]

TABLE 17: C_{70} and Solvent Molecular Parameters Used in the Application of the Gierer and Wartz Model[a]

solvent	V_s (Å^3)	C_o	σ_{GW}	f_{GW}
benzene-d_6	99.5	4.73	0.063	0.297
chlorobenzene-d_5	112.8	4.97	0.058	0.287
o-dichlorobenzene-d_4	125.9	5.21	0.053	0.277

[a] V_s solvent van der Waals volumes were calculated at the 6-31G* level. The value for C_{70} was calculated to be 685.1 Å^3.

$$f_{GW} = \sigma_{GW} C_O \tag{9}$$

where

$$C_O = \left[\frac{6(V_S/V_P)^{0.33}}{(1 + 2(V_S/V_P)^{0.33})^4} + \frac{1}{(1 + 4(V_S/V_P)^{0.33})^3}\right]^{-1} \tag{10}$$

and $\sigma_{GW} = (1 + 6(V_S/V_P)^{1/3}C_o)^{-1}$. A σ_{GW} value of unity indicates the "stick" limit, whereas the "slip" limit is reached when σ_{GW} equals zero. The σ_{GW} factor also provides an indication of the angular velocity coherence between the first solvent shell and the angular velocity of a probe molecule. Essentially, this approach correlates the frictional changes being experienced by a probe to the varying solvent-probe molecular volume ratios, V_S/V_P. Table 17 lists solvent molecular parameters along with calculated C_o, σ_{GW}, and f_{GW} parameters. Solvation values indicate that C_{70} is similarly solvated in these solvents and σ_{GW} suggests that C_{70}'s diffusion is much closer to the slip than the stick limit with the solute−solvent velocity coherence decreasing in the order of BZ > CBZ > DCBZ.

TABLE 18: Experimental and Gierer−Wirtz Predictions of the Rotational Diffusion Rates of C_{70} in Benzene-d_6 at Various Temperatures[a]

		experimental		G−W	
T (K)	h (cP)	$D_Z \times 10^{-10}$ (1/s)	$D_X \times 10^{-10}$ (1/s)	$D_Z \times 10^{-10}$ (1/s)	$D_X \times 10^{-10}$ (1/s)
283	0.755	1.6	0.6	1.6	1.0
293	0.649	1.7	1.2	1.9	1.2
303	0.562	1.9	1.5	2.2	1.4
313	0.492	2.7	2.0	2.6	1.7
323	0.434	3.7	2.4	1	2.0

[a] Solvation parameter, C_o, σ_{GW}, and friction coefficient, f_{GW}, in this solvent were found to be 4.73, 0.063, and 0.297, respectively.

TABLE 19: Experimental and Gierer−Wirtz Predictions of the Rotational Diffusion Rates of C_{70} in Chlorobenzene-d_5 at Various Temperatures[a]

		experimental		G−W	
T (K)	h (cP)	$D_Z \times 10^{-10}$ (1/s)	$D_X \times 10^{-10}$ (1/s)	$D_Z \times 10^{-10}$ (1/s)	$D_X \times 10^{-10}$ (1/s)
283	0.929	1.6	0.8	1.9	1.2
293	0.814	1.6	1.4	2.2	1.4
303	0.719	1.8	1.8	2.6	1.7
313	0.640	2.6	2.3	3.1	1.9
323	0.573	3.9	2.6	3.6	2.2

[a] Solvation parameter, C_o, σ_{GW}, and friction coefficient, f_{GW}, in this solvent were found to be 4.97, 0.058, and 0.287, respectively.

In our previous study, we intuitively modified the Gierer−Wirtz model by proposing that C_{70}'s spinning and tumbling motion could be viewed as being equivalent to the reorientation of spheroids with two different molecular radii.[1] In this modified approach, motion about the *z*-axis, D_Z, is equated to motion of a spheroid of radius r_x; 3.545 Å in C_{70}. For a prolate, motion about the *x* or *y*-axis would correspond to motion of the top axis, r_z, which in C_{70} equals 4.130 Å.

We used the calculated Gierer-Wirtz friction coefficient, f_{GW}, from Table 17 and the appropriate semi-axes values for C_{70} in eq 8 to derive D_Z and D_X values in these solvents at the various temperatures. These predictions are shown in the last two columns of Table 18 − 20.

In benzene, the predicted diffusion constants follow the same trend as was observed experimentally. Model caculated D_Z values are seen to be slightly lower than observed experimentally indicating that C_{70} is spinning faster than predicted. On the other hand, the tumbling motion, D_X, is predicted to be faster at the lowest temperature and is semiquantitative at the remaining temperatures. For both diffusion constants, the agreement between experimental and predicted values is quite good with better agreement being realized with rising temperature. In the case of chlorobenzene, Table 19, the overall concurrence between experiment and predicted values is also acceptable; especially for D_X. The model predicts that C_{70} should be experiencing faster spinning motion in this solvent than observed. One also notices the agreement between model and experimental diffusion constants improve with rising temperature. In DCBZ, Table 20, the predicted diffusions are not quite as good as in the other two solvents. The model predicts that diffusion, about either axis, should experience a higher retardation than is experimentally seen. Consequently, the predicted D_Z values are lower than experiment signifying that C_{70} is spinning much faster than calculated. The calculated D_X values in this solvent do not increase as dramatically with rising temperature, suggesting the model overestimates the role played by solvent's bulk viscosity. Unlike the other two solvents, the agreement between model predictions and experiment worsen with rising temperature indicating the model's ability to characterize diffusion decreases with rising solvent viscosity.

TABLE 20: Experimental and Gierer−Wirtz Predictions of the Rotational Diffusion Rates of C_{70} in *o*-Dichlorobenzene-d_4 at Various Temperatures[a]

		experimental		G−W	
T (K)	h (cP)	$D_Z \times 10^{-10}$ (1/s)	$D_X \times 10^{-10}$ (1/s)	$D_Z \times 10^{-10}$ (1/s)	$D_X \times 10^{-10}$ (1/s)
283	1.404	1.1	0.6	0.9	0.5
293	1.283	1.2	1.2	1.0	0.6
303	1.180	1.5	1.5	1.1	0.7
313	1.080	2.3	1.9	1.2	0.8
323	1.013	3.6	2.1	1.4	0.9

[a] Solvation parameter, C_o, σ_{GW}, and friction coefficient, f_{GW}, in this solvent were found to be 5.21, 0.053, and 0.277, respectively.

Noting that the Gierer−Wirtz approach uses a common friction coefficient (f_{GW}) for the spinning and tumbling motions leads one to propose that separate friction coefficients, one for each type of motion, are necessary to adequately treat the molecular dynamics for these types of molecules. For C_{70}, a fit of our experimental D_Z values to the Gierer−Wartz theory yielded f_{GW} values for the spinning motion of 0.126, 0.122, and 0.065 in benzene, chlorobenzene, and dichlorobenzene, respectively. It is interesting to note that these fitted friction coefficients parallel σ_{GW} values suggesting that σ_{GW} values provide a measure of the rotational "freedom" of a solute in a given solvent and/or of the angular velocity coherence between the solute and the first solvent shell. This observation is consistent with the view that, unlike the tumbling motion, spinning does not require solvent displacement, which results in a lower f_{GW} value. Although spinning does not require solvent displacement, the value for f_{GW} will still reflect the presence or absence of interactions and the degree of rotational freedom that can arise from the ability of the solute to create "cavities" within the solvent.

6. Conclusions

The relaxation measurements indicate that the CSA mechanism dominates the relaxation process at 283 K and decreases with rising temperature. The SR pathway begins to dominate at 323 K. Experimental correlation times, τ_C^{eff}, and diffusion coefficients D_Z and D_X in all solvents showed the overall reorientational motion to be anisotropic at the two extreme temperature but, within experimental error, to be isotropic from 293 to 313 K. When anisotropic, diffusion about the figure axis (i.e., spinning) was seen to be significantly higher than diffusion of the figure axis (i.e., tumbling) indicating the presence of a higher frictional force for the tumbling motion. These measurements indicate that C_{70}'s oscillating behavior, between anisotropic and isotropic molecular reorientation, is not isolated to chlorobenzene but is also exhibited in at least the other two solvents, suggesting that this behavior may be ubiquitous across other solutions.

The theoretical predictions calculated via the modified Gierer−Wirtz model generated diffusion constants that were congruent with the temperature behavior of the experimental values. Predicted D_X values were usually more closely reproduced indicating that the model is better at representing the tumbling motion of a symmetric-top molecule. On the other hand, the approach generally underestimated the D_Z values suggesting that C_{70} is undergoing freer rotation than predicted.

Overall, our data indicate that the factors affecting rotational behavior are complex and that multiple solvent factors are

necessary to characterize the overall rotational motion of C_{70} in these solvents. Although a solvent's viscosity appears to be sufficient to characterize the tumbling behavior, the spinning motion is less sensitive to solvent viscosity but more responsive to solvent structure (e.g., solvent free volume and/or solvent cavities). In fact, according to our experimental fit of the Gierer−Wartz friction coefficients, we estimate that the friction coefficient for the spinning motion to be approximately 2.5 lower than for the tumbling motion. Ultimately, the balance and collective influence of these factors determines the overall rotational behavior.

Acknowledgment. The authors are grateful to the National Science Foundation for support of this project under Grant CH-9707163.

References and Notes

(1) Hughes, R. M.; Mutzenhardt, P.; Bartolotti, L.; Rodriguez, A. A. *J. Mol. Liq*. **2005**, *116*, 139.
(2) Kroto, H. W.; Heath, J. R.; O'Brien, S. C.; Curl, R. F.; Smalley, R. E. *Nature* **1985**, *318*, 162.
(3) Gallagher, S. H.; Armstrong, R. S.; Lay, P. A.; Reed, C. A. *J. Phys. Chem*. **1995**, *99*, 5817.
(4) Chase, B.; Herron, N.; Holler, E. *J. Phys. Chem*. **1992**, *96*, 4262.
(5) Rubtsov, I. V.; Khudiakov, D. V.; Nadtochenko, V. A.; Lobach, A. S.; Moravskii, A. P. *Chem. Phys. Lett*. **1994**, *229*, 517.
(6) Hirsch, A.; Grosser, T.; Skebe, A.; Soi, A. *Chem. Ber*. **1993**, *126*, 1061.
(7) Stokes, G. *Trans. Cambridge Pilos. Soc*. 9 **1856**, 5. Einstein, A. *Investigations on the Theory of the Brownian Movement*; Dover: New York, **1956**. Deby, P. *Polar Molecules*; Dover: New York, **1929**.
(8) Gierer, A.; Wirtz, K. *Z. Naturforsch*. **1953**, *A8*, 532.
(9) Hynes, J. T.; Kapral, R.; Weinberg, M. *Chem. Phys. Lett*. **1977**, *47*, 575.
(10) Hynes, J. T.; Kapral, R.; Weinberg, M. *J. Chem. Phys*. **1978**, *69* (6), 2725.
(11) Hynes, J. T.; Kapral, R.; Weinberg, M. *J. Chem. Phys*. **1977**, *67* (7), 3256.
(12) Hu, C.-M.; Zwanzig, R. *J. Chem. Phys*. **1974**, *60* (11), 4354.
(13) Youngren, G. K.; Acrivos, A. *J. Chem. Phys*. **1975**, *63* (9), 3846.
(14) Froimowitz, M. *J. Comput. Chem.* **1991**, *12*, 1129.
(15) Baker, J.; Fowler, P. W.; Lazzeretti, P.; Malagoli, M.; Zanasi, R. *Chem. Phys. Lett*. **1991**, *184* (1−3), 182.
(16) Jones, V. K.; Rodriguez, A. A. *Chem. Phys. Lett*. **1992**, *198*, 373.
(17) Shang, X.; Fisher, L. A.; Rodriguez, A. A. *J. Phys. Chem*. **1996**, *100*, 4361.
(18) Jones, J. A.; Rodriguez, A. A. *Chem. Phys. Lett*. **1994**, *230*, 160.
(19) Shang, X.; Rodriguez, A. A.; *J. Phys. Chem. A* **1997**, *101*, 103.
(20) Martin, N. H.; Issa, M. H.; McIntyre, R. A.; Rodriguez, A. A. *J. Phys. Chem. A* **2000**, *104*, 11278.
(21) Irwin, A. D.; Assink, R. A.; Henderson, C. C.; Cahill, P. A. *J. Phys. Chem*. **1994**, *98*, 11832.
(22) Rubtsov, I. V.; Khudakov, D. V.; Nadtochenko, V. A.; Lobach, V. A.; Moravskii, A. P. *Chem. Phys. Lett*. **1994**, *229*, 517.
(23) Aldrich Chemical Company, Milwaukee, WI, 53233.
(24) Korobov, M. V.; Smith, A. L. In *Fullerenes: Chemistry, Physics, and Technology*; Kadish, K. M., Ruoff, R. S., Ed.s; Wiley: New York, 2000; p 53.
(25) Yannoni, C. S.; Johnson, R. D.; Meijer, G.; Bethune, D. S.; Salem, J. R. *J. Phys. Chem*. **1991**, *95*, 9.
(26) Walton, J. H.; Kamasa-Quashie, A. K.; Joers, J. M.; Gullion, T. *Chem. Phys. Lett*. **1993**, *203* (2,3), 237.
(27) Johnson, R. D.; Yannoni, C. S.; Dorn, H. C.; Salem, J. R.; Bethune, D. S. *Science* **1992**, *255*, 1235.
(28) Dorn, H. C.; Gu, J.; Bethune, D. S.; Johnson, R. D.; Yannoni, C. S. *Chem. Phys. Lett*. **1993**, *203* (5,6), 549.
(29) Becker, E. D. *High-Resolution NMR: Theory and Applications*, 2nd ed.; Academic Press: New York, 1980.
(30) Abragam, A. *The Principals of Nuclear Magnetism*; Oxford University Press: New York, 1961.
(31) Tycko, R.; Dabbagh, G.; Vaughan, G. B. M.; Cichy, M. A.; Heiney, P. A.; Strongin, R. M.; Smith, A. B. *J. Chem. Phys*. **1993**, *99* (10), 7554.
(32) Walker, O.; Mutzenhardt, P.; Tekely, P.; Canet, D. *J. Am. Chem. Soc*. **2002**, *24* (5), 865.
(33) Bryce, D. L.; Wasylishen, R. E. *Phys. Chem. Chem. Phys*. **2002**, *4*, 3591.
(34) Facelli, J. C.; Nakagawa, B. K.; Orendt, A. M.; Pugmire, R. J. *J. Phys. Chem. A* **2001**, *105*, 7468.
(35) Latosinska, J. N. *J. Mol. Struct*. **2003**, *646*, 211.
(36) Colhoun, F. L.; Armstrong, R. C.; Rutledge, G. C. *Polymer* **2002**, *43*, 609.
(37) Stueber, D.; Grant, D. M. *Solid State NMR* **2002**, *22*, 439.
(38) Zheng, G.; Hu, J.; Zhang, X.; Shen, L.; Ye, C.; Webb, G. A. *Chem. Phys. Lett*. **1997**, *266*, 533.
(39) Malkin, V. G.; Malkina, O. L.; Salahub, D. R. *J. Am. Chem. Soc*. **1995**, *117*, 3294.
(40) Frisch, M. J.; Trucks, G. W.; Schlegel, H. B.; Scuseria, G. E.; Robb, M. A.; Cheeseman, J. R.; Zakrzewski, V. G.; Montgomery, J. A., Jr.; Stratmann, R. E.; Burant, J. C.; Dapprich, S.; Millam, J. M.; Daniels, A. D.; Kudin, K. N.; Strain, M. C.; Farkas, O.; Tomasi, J.; Barone, V.; Cossi, M.; Cammi, R.; Mennucci, B.; Pomelli, C.; Adamo, C.; Clifford, S.; Ochterski, J.; Petersson, G. A.; Ayala, P. Y.; Cui, Q.; Morokuma, K.; Malick, D. K.; Rabuck, A. D.; Raghavachari, K.; Foresman, J. B.; Cioslowski, J.; Ortiz, J. V.; Baboul, A. G.; Stefanov, B. B.; Liu, G.; Liashenko, A.; Piskorz, P.; Komaromi, I.; Gomperts, R.; Martin, R. L.; Fox, D. J.; Keith, T.; Al-Laham, M. A.; Peng, C. Y.; Nanayakkara, A.; Challacombe, M.; Gill, P. M. W.; Johnson, B.; Chen, W.; Wong, M. W.; Andres, J. L.; Gonzalez, C.; Head-Gordon, M.; Replogle, E. S.; Pople, J. A. *Gaussian 98*, revision A.9; Gaussian, Inc.: Pittsburgh, PA, 1998.
(41) Becke, A. D. *J. Chem. Phys*. **1993**, *98*, 5648.
(42) Lee, C.; Yang, W.; Parr, R. G. *Phys. Rev. B* **1988**, *37*, 785.
(43) McWeeny, R. *Phys. Rev*. **1959**, *114*, 1528.
(44) Ditchfield, R. *Mol. Phys*. **1974**, *27*, 789.
(45) Dodds, J. L.; McWeeny, R.; Sadlej, A. *J. Mol. Phys*. **1980**, *41*, 1419.
(46) Wolinski, K.; Hilton, J. F.; Pulay, P. *J. Am. Chem. Soc*. **1990**, *112*, 8251−8260.
(47) Bloembergen, N.; Purcell, E. M.; Pound, R. V. *Nature* **1947**, *160*, 475.
(48) Bloembergen, N. *Nuclear Magnetic Resonance*; W. A. Benjamin: New York, 1969.
(49) Huntress, W. T. *Advances in Magnetic Resonance*; Academic Press: New York, 1971; Vol. 4.
(50) Gallagher, S. H.; Armstrong, R. S.; Lay, P. A.; Reed, C. A. *Chem. Phys. Lett*. **1996**, *248*, 353.
(51) Gallagher, S. H.; Armstrong, R. S.; Lay, P. A.; Reed, C. A. *J. Phys. Chem*. **1995**, *99*, 5817.
(52) The Hildebrand−Batschinski equation was employed to calculate the rotational space available to C_{70} in benzene, chlorobenzene, and *o*-dichlorobenzene. The average volumes were found to be 497, 421, and 225 $Å^3$, respectively.
(53) Parrin, E. *J. Phys. Radium* **1932**, *5*, 497.
(54) Gillen, K. T.; Griffiths, J. E. *Chem. Phys. Lett*. **1972**, *17*, 359.
(55) Dote, J. L.; Kivelson, D.; Schwartz, R. N. *J. Phys. Chem*. **1981**, *85*, 2169.